

Structural Analysis of Directional qLDPC Codes

Mohammad Rowshan^{1,*}

¹University of New South Wales (UNSW), Kensington, NSW 2052, Australia

(Dated: February 24, 2026)

Directional codes, recently introduced by Gehér–Byfield–Ruban [1], constitute a hardware-motivated family of quantum low-density parity-check (qLDPC) codes. These codes are defined by stabilizers measured by ancilla qubits executing a fixed *direction word* (route) on square- or hex-grid connectivity. In this work, we develop a comprehensive *word-first* analysis framework for route-generated, translation-invariant CSS codes on rectangular tori. Under this framework, a direction word W deterministically induces a finite support pattern $P(W)$, from which we analytically derive: (i) a closed-form route-to-support map; (ii) the odd-multiplicity difference lattice $L(W)$ that classifies commutation-compatible X/Z layouts; and (iii) conservative finite-torus admissibility criteria. Furthermore, we provide: (iv) a rigorous word equivalence and canonicalization theory (incorporating dihedral lattice symmetries, reversal/inversion, and cyclic shifts) to enable symmetry-quotiented searches; (v) an “inverse problem” criterion to determine when a translation-invariant support pattern is realizable by a single route, including reconstruction and non-realizability certificates; and (vi) a quasi-cyclic (group-algebra) reduction for row-periodic layouts that explains the sensitivity of code dimension k to boundary conditions. As a case study, we analyze the word $W = \text{NE}^2\text{NE}^2\text{N}$ end-to-end. We provide explicit stabilizer dependencies, commuting-operator motifs, and an exact criterion for dimension collapse on thin rectangles: for $(L_x, L_y) = (2d, d)$ with row alternation, we find $k = 4$ if $6 \mid d$, and $k = 0$ otherwise.

I. INTRODUCTION

Quantum error correction (QEC) enables reliable quantum computation by encoding logical information into many physical qubits. The stabilizer and CSS frameworks convert QEC into linear-algebraic constraints over \mathbb{F}_2 [2–5]. In classical coding theory, low-density parity-check (LDPC) codes are defined by sparse parity-check graphs and admit efficient iterative decoding [6–8]. Quantum LDPC (qLDPC) codes adapt this sparsity to the stabilizer setting [9–11].

A practical issue is that “good” asymptotic qLDPC parameters do not automatically imply implementable layouts. Two-dimensional topological codes such as toric and surface codes have strictly local checks and mature decoders [12–14], but 2D locality imposes strong scaling constraints [15, 16]. Meanwhile, many powerful qLDPC constructions (products, Cayley/expander ideas, asymptotically good families) are not natively aligned with strict 2D connectivity [17–24]. Recent progress shows that algebraic structure can be paired with engineering constraints: bivariate bicycle codes demonstrate high thresholds and low overhead [25] and motivate architectural proposals [26], while connectivity-reduction techniques such as morphing circuits [27] and hardware-aware placement/routing studies [28, 29] further emphasize co-design.

Directional codes, introduced in [1], take the co-design philosophy to an extreme: the stabilizer support is generated by a short *direction word* (a route) that every ancilla follows on a low-degree lattice. This route-generated restriction makes strict square/hex connectivity natural, but it also introduces delicate structural dependence on the word and on boundary conditions: small changes in W can alter (i) which X/Z layouts are allowed, (ii) which finite tori admit collision-free schedules, and (iii) which boundary conditions preserve or collapse the dimension k .

A. Relationship to the seminal work and contributions

The construction and core layout-classification mechanism are due to Gehér–Byfield–Ruban [1]. Sections II–III represent these foundational ingredients from [1] in a word-centric language with explicit examples and diagrams (route-to-support formula; odd-multiplicity lattice governing commutation-compatible layouts; conservative finite-torus admissibility filters). The contributions of this work begin in Sections IV–IX:

1. *Word equivalence and canonical representatives* (Sec. IV): we formalize an equivalence group generated by dihedral lattice symmetries, reversal with inversion, and cyclic shifts, prove that it induces code isomorphisms on compatible tori, and give a canonicalization procedure for symmetry-quotiented searches.

* m.rowshan@unsw.edu.au

2. *The route realizability inverse problem* (Sec. V): given a translation-invariant offset set P , when does there exist a single direction word W such that $P = P(W)$? We give a reconstruction criterion and practical non-realizability certificates.
3. *A quasi-cyclic (group-algebra) reduction for row-periodic layouts* (Sec. IX): for common layouts such as row alternation, we reduce stabilizer-dependency and rank questions to annihilator computations in a small polynomial ring. As an application we prove an exact divisibility criterion explaining the observed k -collapse for $W = \text{NE}^2\text{NE}^2\text{N}$ on thin rectangles (Theorem 4).

B. Outline

Section II develops the checkerboard model and the route-to-support map. Section III introduces the odd-multiplicity difference lattice and its layout classification theorem. Section IV develops word symmetries and canonicalization. Section V treats the inverse problem of route realizability. Section VI discusses finite-torus admissibility and introduces the polynomial/QC viewpoint, while Section IX develops the row-periodic annihilator formalism. Section X provides worked families and a detailed case study. Section XI documents the reproducible numerical pipeline and representative scans [30]. Finally, Section XII summarizes and discusses future directions.

II. CHECKERBOARD MODEL AND ROUTE-GENERATED CHECKS (AFTER [1])

We adopt the standard CSS setting [3–5], but present it in the coordinate system that makes directional codes convenient to compute with.

A. CSS codes and parameters

A CSS code is specified by two binary matrices H_X, H_Z with $H_X H_Z^T = 0$. The number of logical qubits is

$$k = n - \text{rank}(H_X) - \text{rank}(H_Z), \quad (1)$$

and the (static) distances are

$$d_X = \min\{\text{wt}(x) : x \in \ker(H_Z) \setminus \text{row}(H_X)\}, \quad (2)$$

$$d_Z = \min\{\text{wt}(z) : z \in \ker(H_X) \setminus \text{row}(H_Z)\}, \quad (3)$$

with $d = \min(d_X, d_Z)$.

B. Checkerboard torus and layouts

We work in 2D grid $G = \mathbb{Z}_{L_x} \times \mathbb{Z}_{L_y}$ with L_x, L_y even, to make the checkerboard split perfectly balanced. Here, \mathbb{Z}_L denotes integers modulo of L (that is, $0, 1, \dots, L-1$ with wraparound). Since the grid “wraps” in both directions x, y , it is a torus topology. We split sites by parity

$$\Lambda_Q = \{(x, y) \in G : x + y \equiv 0 \pmod{2}\} \quad (\text{data}), \quad (4)$$

$$\Lambda_A = \{(x, y) \in G : x + y \equiv 1 \pmod{2}\} \quad (\text{ancilla}). \quad (5)$$

Thus, $|\Lambda_Q| = |\Lambda_A| = n = \frac{1}{2}L_x L_y$. A *layout* is a partition $\Lambda_A = \Lambda_X \sqcup \Lambda_Z$; every ancilla site will be assigned to measure either an X-check (goes in Λ_X), or a Z-check (goes in Λ_Z). Equivalently, a label function $\alpha : \Lambda_A \rightarrow \{X, Z\}$ tells you the check type for each ancilla site. Figure 1 illustrates an example layout for $G = \mathbb{Z}_8 \times \mathbb{Z}_6$. On a checkerboard lattice, data qubits live on one sublattice, and ancillas live on the other sublattice.

C. Direction words and compressed notation

A *direction word* is a string $W = d_1 d_2 \cdots d_w$ with letters from $\mathcal{D} = \{N, E, S, W\}$, interpreted as steps

$$N = (0, 1), \quad E = (1, 0), \quad S = (0, -1), \quad W = (-1, 0).$$

We also use a compact notation: for example NE^2N means N E E N , and $\text{NE}^2\text{NE}^2\text{N}$ means N E E N E E N .

Z	•	Z	•	Z	•	Z	•
•	X	•	X	•	X	•	X
Z	•	Z	•	Z	•	Z	•
•	X	•	X	•	X	•	X
Z	•	Z	•	Z	•	Z	•
•	X	•	X	•	X	•	X

FIG. 1. Checkerboard data/ancilla partition (shown as a patch) and a simple example layout with row alternation. Here, black dots are data qubits ($x + y$ even) and X/Z labels mark ancillas ($x + y$ odd).

D. From a word to a support pattern

Let the partial sums $S_j = \sum_{t=1}^j d_t$ with $S_0 = (0, 0)$ be the running “walk location”, which gives the position after j steps, if you start at the origin. For example, after step 1, you are at $S_1 = d_1$, after step 2 you are at $S_2 = d_1 + d_2$, etc.

In directional codes, the order in which an ancilla interacts with data qubits follows a fixed route on the lattice. At each step, the data qubit involved depends only on the ancilla’s position before and after that step. Because these data qubits lie halfway between consecutive route positions, we multiply coordinates by two so that all positions are integers. This leads to a simple formula that directly gives the data-qubit location for each step.

Lemma 1 (Route-to-offset formula). *Define integer offsets*

$$Q_j = S_{j-1} + S_j = 2 \sum_{t=1}^{j-1} d_t + d_j, \quad j = 1, \dots, w. \quad (6)$$

Then an ancilla anchored at $a \in \Lambda_A$ interacts with data qubits at sites $a + Q_j \pmod{G}$.

Remark 1 (Route interpretation as a local-gate schedule). Although a direction word is drawn as a geometric route, no qubit is physically transported across the lattice. Instead, the word specifies a *sequence of local two-qubit interactions* that propagates the ancilla’s *quantum state* along nearest-neighbor edges. Data qubits remain fixed, and each interaction is local in the underlying connectivity graph. Directional codes thus trade strict geometric locality of a single stabilizer (as in plaquette codes) for a fixed, bounded-depth measurement schedule compatible with low-degree hardware graphs [1].

Definition 1 (Support pattern). The support pattern of W is the set

$$P(W) = \{Q_1, \dots, Q_w\} \subset \mathbb{Z}^2, \quad (7)$$

understood modulo (L_x, L_y) when embedded in G . A directional check anchored at a acts on data qubits in the translated support $a + P(W)$.

Note that the shifted (translated) locations of the offset set $P(W)$ by the anchor position a are the data qubits included in the stabilizer check. Thus, W gives the shape and a gives the placement.

The construction becomes conceptually simple: *choosing W chooses $P(W)$* , hence fixes the check shape (up to translation), and the remaining degrees of freedom are (i) the layout (which ancillas are X or Z) and (ii) the boundary conditions (the torus vectors).

a. Pattern-code viewpoint. Once $P(W)$ is fixed, directional codes fit inside translation-invariant *pattern CSS codes*:

$$S_a^X = \prod_{q \in a + P(W)} X_q, \quad a \in \Lambda_X, \quad (8)$$

$$S_b^Z = \prod_{q \in b + P(W)} Z_q, \quad b \in \Lambda_Z, \quad (9)$$

where Λ_X, Λ_Z form a partition of the ancillas (the *layout*).

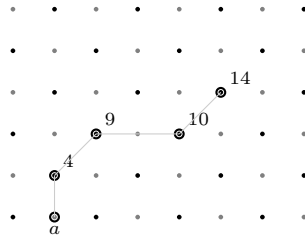


FIG. 2. Toy instance illustrating the terminology. Gray sites are ancillas, black sites are data. For $W = \text{NE}^2\text{N}$ and anchor $a = (1, 0)$ the four circled data qubits are the translated support $a + P(W)$.

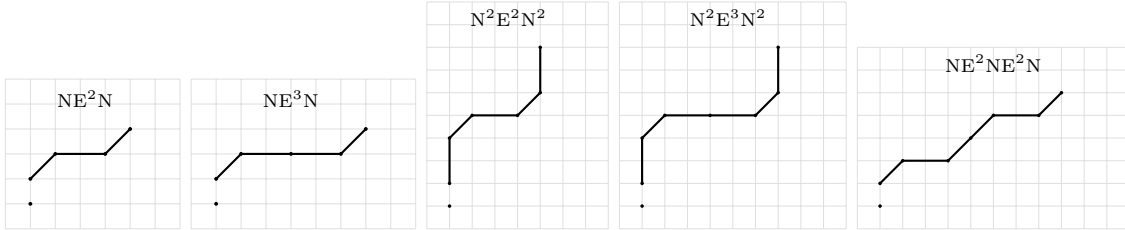


FIG. 3. Support patterns $P(W)$ for five representative words, plotted as integer offsets relative to an ancilla anchor at the origin.

Remark 2. We cover the whole grid by translating the same route-defined check to every ancilla position. The union of all translated supports $\bigcup_{a \in \Lambda_A} (a + P(W))$ spreads across the entire data lattice, so every data qubit participates in checks.

Example 1 (word \rightarrow check *and* a row of H).

$$P(W) = \{(0, 1), (1, 2), (3, 2), (4, 3)\},$$

where the offsets are obtained as $Q_1 = S_0 + S_1 = (0, 0) + (0, 1) = (0, 1)$, $Q_2 = S_1 + S_2 = (0, 1) + (1, 1) = (1, 2)$, etc. For the anchor $a = (1, 0) \in \Lambda_A$, the translated support is

$$a + P(W) = \{(1, 1), (2, 2), (4, 2), (5, 3)\} \subset \Lambda_Q,$$

where $x + y$ is even parity for all positions. If we index data qubits in lexicographic order by looping over rows increasing $y = 0, 1, \dots, 5$, and inside each row, looping over columns in increasing $x = 0, 1, \dots, 7$ (*skipping* ancilla sites), considering only sites where $x + y$ is even, these coordinates correspond to column indices $\{4, 9, 10, 14\}$ of H . Therefore, the parity-check row contributed by this ancilla is

$$h_a = e_4 + e_9 + e_{10} + e_{14} \in \mathbb{F}_2^n.$$

Figure 2 shows this translation geometrically. To get the entire H matrix, Loop over all ancillas $a \in \Lambda_A$ and place that row in H_X if $\alpha(a) = X$ or H_Z if $\alpha(a) = Z$. Stack all rows and we get $|\Lambda_A| = 24$ rows where each row has weight $w = 4$ for NE^2N .

E. Representative support patterns

Figure 3 shows $P(W)$ for five representative words. The first four are benchmark examples in [1]; the fifth is our case study.

III. LAYOUT CLASSIFICATION VIA ODD-MULTIPLICITY DIFFERENCES (AFTER [1])

Directional codes impose a global constraint: not every layout α is compatible with a given W . The mechanism is overlap parity: an X -check and a Z -check anticommute iff they overlap on an odd number of data qubits. Since all checks share the same shape $P(W)$ up to translation, overlap parity depends only on the displacement between anchors. This section turns that intuition into a computable invariant.

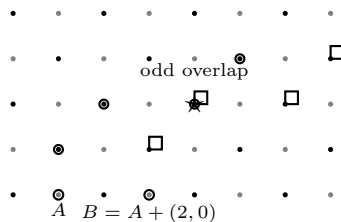


FIG. 4. For $W = \text{NE}^2\text{N}$, anchors separated by $\delta = (2, 0)$ have supports that overlap on exactly one data qubit (star). Thus $\delta = (2, 0)$ forbids assigning opposite types to those ancillas. This is the concrete meaning of an “odd-difference” displacement.

A. Odd-multiplicity differences and the forced-equality lattice

Let $P(W) = \{Q_1, \dots, Q_w\}$. Define the difference multiset

$$\Delta(W) = \{v = Q_j - Q_i : 1 \leq i < j \leq w\}, \quad (10)$$

with multiplicity $\mu(v)$ counting how many pairs yield the same v .

Definition 2 (Odd-multiplicity difference set and lattice). Define

$$\Delta_{\text{odd}}(W) = \{v \in \mathbb{Z}^2 : \mu(v) \equiv 1 \pmod{2}\}, \quad (11)$$

and the *odd-multiplicity difference lattice*

$$L(W) = \text{span}_{\mathbb{Z}}(\Delta_{\text{odd}}(W)). \quad (12)$$

Remark 3 (Intuition for $L(W)$). Suppose a displacement δ is “forbidden” (i.e., it produces an odd overlap). Then ancillas at a and $a + \delta$ are not allowed to have opposite types, so they must share the same label. Applying the same rule repeatedly shows that ancillas at $a, a + \delta, a + 2\delta, a + 3\delta, \dots$ must all have the same label; in other words, labels are constant along all integer multiples of δ . If there are several forbidden displacements, the same chaining works for any sum of them. Therefore we collect all integer combinations of forbidden displacements into the lattice $L(W) = \text{span}_{\mathbb{Z}}(\Delta_{\text{odd}}(W))$, and $L(W)$ is exactly the set of displacements along which ancilla labels are forced to be equal.

B. Worked example: computing Δ_{odd} and $L(W)$

Example 2 (computing Δ_{odd} for NE^2N). For $W = \text{NE}^2\text{N}$, we have $P(W) = \{(0, 1), (1, 2), (3, 2), (4, 3)\}$. Computing all $Q_j - Q_i$ with $j > i$, we get $Q_2 - Q_1 = (1, 1)$, $Q_3 - Q_1 = (3, 1)$, $Q_4 - Q_1 = (4, 2)$, $Q_3 - Q_2 = (2, 0)$, $Q_4 - Q_2 = (3, 1)$, and $Q_4 - Q_3 = (1, 1)$. The differences include $(2, 0)$ and $(4, 2)$ exactly once each, while $(1, 1)$ and $(3, 1)$ occur twice. Thus, the forbidden ancilla displacements are

$$\Delta_{\text{odd}}(\text{NE}^2\text{N}) = \{(2, 0), (4, 2)\}.$$

Take integer combinations, including subtractions

$$m(2, 0) + n(4, 2) = (2m + 4n, 2n),$$

and rewrite it as

$$(2(m + 2n), 2n) = (2k, 2\ell),$$

where $k = m + 2n$ and $\ell = n$. Then all vectors have even x and y . So, a basis for $L(W)$ can be

$$L(\text{NE}^2\text{N}) = \text{span}_{\mathbb{Z}}\{(2, 0), (4, 2)\} = 2\mathbb{Z} \times 2\mathbb{Z}.$$

From the above basis, $(4, 2) - 2(2, 0) = (4, 2) - (4, 0) = (0, 2)$. Physically, if the ancillas at distance $(4, 2)$ must agree, and the ancillas at distance $(2, 0)$ must agree, then the ancillas at distance $(0, 2)$ must also agree. That is transitivity.

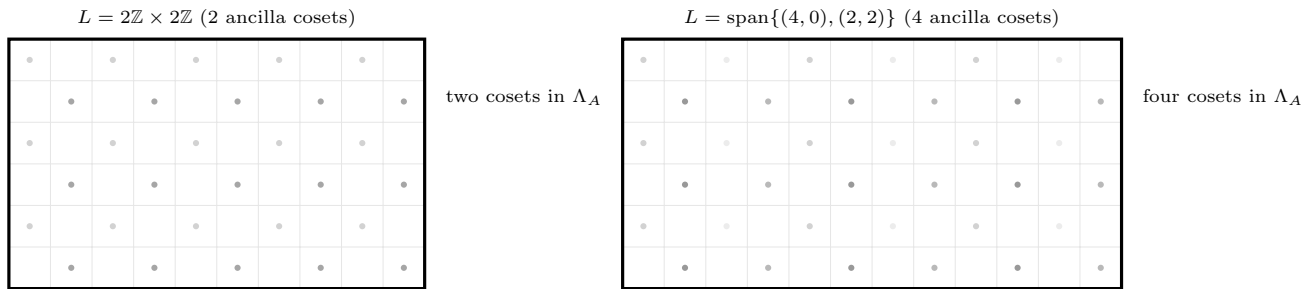


FIG. 5. Coset structure on ancillas for two lattice types that occur frequently in directional-code words. A layout is any X/Z labeling constant on these cosets (Theorem 1).

TABLE I. Odd-multiplicity invariants for representative words (computed from $P(W)$).

Word W	w	$\Delta_{\text{odd}}(W)$ (generators shown)	basis for $L(W)$	$[\mathbb{Z}^2 : L(W)]$	ancilla cosets
NE^2N	4	$\{(2, 0), (4, 2)\}$	$\{(2, 0), (0, 2)\}$	4	2
NE^3N	5	$\{(4, 0), (6, 2)\}$	$\{(4, 0), (2, 2)\}$	8	4
$\text{N}^2\text{E}^2\text{N}^2$	6	$\{(2, 0), (4, 2), (4, 6)\}$	$\{(2, 0), (0, 2)\}$	4	2
$\text{N}^2\text{E}^3\text{N}^2$	7	$\{(4, 0), (6, 2), (6, 6)\}$	$\{(4, 0), (2, 2)\}$	8	4
$\text{NE}^2\text{NE}^2\text{N}$	7	$\{(2, 2), (6, 2), (8, 4)\}$	$\{(4, 0), (2, 2)\}$	8	4

Figure 4 geometrically illustrates the odd-overlap displacement $(2, 0)$ in this set.

Remark 4 (Choosing a basis for $L(W)$). To extract a convenient basis for a given $\Delta_{\text{odd}}(W)$, one may freely add or subtract integer multiples of generators, since such operations do not change the lattice. In practice, this reduction typically yields a simple rank-two basis consisting of a “horizontal” vector $(d, 0)$ and a “diagonal” or “vertical” vector (e, f) , or, after further simplification, purely horizontal and vertical vectors such as $(d, 0)$ and $(0, f)$. The particular choice of basis is not unique; any pair of independent integer vectors generating the same lattice is equally valid.

C. Layout coset theorem

Theorem 1 (Layout coset theorem). *Fix a direction word W on the infinite checkerboard lattice. Any layout $\alpha : \Lambda_A \rightarrow \{X, Z\}$ compatible with directional-code commutation/scheduling constraints must be constant on cosets of $L(W)$:*

$$a - b \in L(W) \Rightarrow \alpha(a) = \alpha(b). \quad (13)$$

Conversely, any layout that is constant on cosets of $L(W)$ yields a translation-invariant CSS commutation pattern for checks generated by $P(W)$.

D. Coset structure for the two principal lattices

The two lattice types that arise repeatedly for the benchmark words are illustrated in Fig. 5. Layouts correspond to choosing X/Z labels constant on these cosets.

E. Invariant summary table for representative words

Table I summarizes $\Delta_{\text{odd}}(W)$ and a convenient basis for $L(W)$ for the five representative words in Fig. 3.

IV. WORD SYMMETRIES AND CANONICAL REPRESENTATIVES

When scanning words, it is important to quotient by symmetries that only relabel the lattice. Let D_4 be the dihedral symmetry group of the square, acting on directions by rotations/reflections. Also consider reversal with

direction inversion, and cyclic shifts.

Definition 3 (Word equivalence). Two words W, W' are equivalent ($W \sim W'$) if they are related by a composition of: (i) a dihedral action on $\{N, E, S, W\}$, (ii) reversal with direction inversion ($N \leftrightarrow S, E \leftrightarrow W$), and (iii) a cyclic shift of letters.

Proposition 1 (Equivalence induces code isomorphism). *If $W \sim W'$, then $P(W')$ is an affine image of $P(W)$ under a lattice automorphism and translation. On any compatible torus embedding, the corresponding directional codes are isomorphic (qubit relabeling and stabilizer relabeling).*

A. Canonicalization procedure for symmetry-quotiented searches

For implementation and numerical searches [30], it is convenient to map each equivalence class to a single *canonical representative*. One simple method is: generate all words in the orbit of W under the finite group generated by the operations in Definition 3, then choose the lexicographically smallest expanded-letter string (ties broken deterministically). A detailed description and complexity bound are given in Appendix D.

V. ROUTE REALIZABILITY AND THE INVERSE PROBLEM

Directional codes form a strict subclass of translation-invariant pattern CSS codes: not every finite offset set P is realizable as $P(W)$ for a *single* route W . This becomes relevant when comparing directional codes to other quasi-cyclic constructions or when proposing a support pattern first and asking whether it admits a directional extraction schedule.

A. A two-step difference identity

Let $Q_j = S_{j-1} + S_j$ as in Lemma 1. Then consecutive offsets satisfy

$$Q_{j+1} - Q_j = d_j + d_{j+1}. \quad (14)$$

Thus, consecutive offsets differ by the sum of two cardinal steps.

Define the finite “two-step difference alphabet”

$$\Sigma := \{u + v : u, v \in \mathcal{D}\} = \{(\pm 2, 0), (0, \pm 2), (\pm 1, \pm 1)\}.$$

B. Route reconstruction and non-realizability certificates

Proposition 2 (Route reconstruction and realizability test). *Let $P \subset \mathbb{Z}^2$ be a multiset of size w . An ordering Q_1, \dots, Q_w of P is realizable by a direction word $W = d_1 \cdots d_w$ with $P(W) = P$ (in that order) if and only if:*

1. $Q_1 \in \mathcal{D}$ (the first offset must be a cardinal step), and
2. for each j , $\Delta_j := Q_{j+1} - Q_j \in \Sigma$, and the recursion

$$d_1 := Q_1, \quad d_{j+1} := \Delta_j - d_j \quad (15)$$

produces letters $d_2, \dots, d_w \in \mathcal{D}$.

If these conditions hold, the reconstructed word is unique for the chosen ordering.

Example 3 (A simple non-realizable offset set). Consider $P = \{(1, 2), (3, 2), (5, 2)\}$. Every point has odd parity ($x + y$ odd), so parity alone does not forbid it, but $P \cap \mathcal{D} = \emptyset$ so no ordering can satisfy $Q_1 \in \mathcal{D}$. Hence P cannot be realized by a single route, even though it is a plausible translation-invariant check pattern. Fig. 6 illustrates this example.

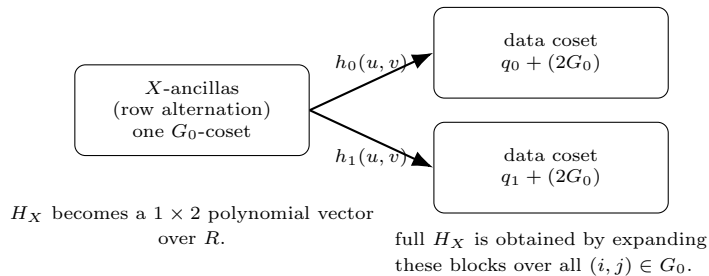


FIG. 8. Row alternation makes Λ_X a single G_0 -coset and Λ_Q the disjoint union of two G_0 -cosets. Consequently, H_X has a block-circulant form generated by a *small* 1×2 polynomial vector $(h_0, h_1) \in R^{1 \times 2}$.

VII. QUASI-CYCLIC RANK PREDICTION AND BOUNDARY-CONDITION SENSITIVITY

Directional codes are translation-invariant in the sense that every check is a translate (shifted copy) of the same finite pattern $P(W)$. This makes the check matrices block-circulant, so questions about $\text{rank}(H_X), \text{rank}(H_Z)$ (hence k) can be reduced to algebra in a small quotient ring. The main takeaway is that *boundary-condition sensitivity of k is not mysterious*: it corresponds to whether certain low-degree polynomials divide the torus relations, a fact that becomes explicit in the quasi-cyclic (QC) representation.

A. Coarse coordinates and a block-circulant normal form

We keep the checkerboard torus $G = \mathbb{Z}_{L_x} \times \mathbb{Z}_{L_y}$ with L_x, L_y even. Translations by *even* vectors preserve the data/ancilla bipartition. Let

$$G_0 := \mathbb{Z}_{L_x/2} \times \mathbb{Z}_{L_y/2},$$

which parametrizes even translations via $(i, j) \mapsto (2i, 2j)$. Each parity class in G (e.g. data sites with $(x, y) \equiv (0, 0) \pmod{2}$) is a torsor for G_0 .

We now fix four base sites:

$$a_X := (1, 0) \in \Lambda_A, \quad a_Z := (0, 1) \in \Lambda_A, \quad q_0 := (0, 0) \in \Lambda_Q, \quad q_1 := (1, 1) \in \Lambda_Q.$$

Then every X -ancilla under row alternation (y even) can be written uniquely as $a_X + (2i, 2j)$ with $(i, j) \in G_0$, and every Z -ancilla (y odd) as $a_Z + (2i, 2j)$. Likewise, every data qubit lies either in the q_0 -coset or the q_1 -coset:

$$q_0 + (2i, 2j) \quad \text{or} \quad q_1 + (2i, 2j), \quad (i, j) \in G_0.$$

Definition 4 (QC ring). Let

$$R := \mathbb{F}_2[u^{\pm 1}, v^{\pm 1}] / (u^{L_x/2} - 1, v^{L_y/2} - 1).$$

We identify functions on G_0 with elements of R in the usual way: the monomial $u^i v^j$ denotes the indicator at $(i, j) \in G_0$ (extended periodically).

B. From a word to a polynomial check vector

Fix a word W and its support pattern $P(W) \subset \mathbb{Z}^2$ (Definition in Sec. II). For each offset $Q = (Q_x, Q_y) \in P(W)$, consider the translate $a_X + Q$. Since $a_X \in \Lambda_A$ and Q has odd parity, $a_X + Q \in \Lambda_Q$. Moreover, $a_X + Q$ lands in exactly one of the two data cosets $q_0 + (2G_0)$ or $q_1 + (2G_0)$, depending on $(Q_x, Q_y) \pmod{2}$.

Definition 5 (Row-alternating QC check vector). For each $Q \in P(W)$, define $(\sigma(Q), \delta(Q))$ as follows:

- $\sigma(Q) \in \{0, 1\}$ is the unique index such that $a_X + Q \in q_{\sigma(Q)} + (2G_0)$;

• $\delta(Q) = (\delta_x(Q), \delta_y(Q)) \in G_0$ is defined by

$$a_X + Q = q_{\sigma(Q)} + (2\delta_x(Q), 2\delta_y(Q)) \quad \text{in } G.$$

Define two polynomials in R by

$$h_\sigma(u, v) := \sum_{Q \in P(W): \sigma(Q)=\sigma} u^{\delta_x(Q)} v^{\delta_y(Q)} \in R, \quad \sigma \in \{0, 1\}.$$

We call $(h_0, h_1) \in R^{1 \times 2}$ the *QC check vector* of $(W, \text{row alternation})$ relative to the chosen bases.

Proposition 4 (Block-circulant expansion). *Under row alternation, the X -check matrix H_X is the block-circulant matrix obtained by expanding the 1×2 polynomial vector (h_0, h_1) over G_0 as in Fig. 8. Equivalently, identifying row coefficients on Λ_X with $f \in R$, the resulting syndrome-on-data vector is*

$$f \cdot (h_0, h_1) = (fh_0, fh_1) \in R \oplus R,$$

where multiplication is in R . An analogous statement holds for H_Z with (h_0, h_1) replaced by the corresponding (g_0, g_1) computed from the base ancilla a_Z .

C. Dependencies as an annihilator module and a computable k -formula

Because we use *every* ancilla as a check (either X or Z), we have $m_X + m_Z = |\Lambda_A| = n$ rows total. Thus, in this model the logical dimension k is exactly the total number of independent stabilizer dependencies.

Proposition 5 (Logical dimension equals number of stabilizer dependencies). *For any commuting CSS instance built on the checkerboard torus with one check per ancilla site,*

$$k = \dim \ker(H_X^\top) + \dim \ker(H_Z^\top).$$

In the QC normal form, these dependency dimensions become small-ring kernel dimensions.

Theorem 2 (QC dependency module for row alternation). *Let $(h_0, h_1) \in R^{1 \times 2}$ be the QC check vector for H_X (Definition 5). Then*

$$\ker(H_X^\top) \cong \{f \in R : fh_0 = 0 \text{ and } fh_1 = 0\}.$$

In particular,

$$\dim \ker(H_X^\top) = \dim_{\mathbb{F}_2} \text{Ann}_R(h_0, h_1),$$

where $\text{Ann}_R(h_0, h_1) = \{f \in R : fh_0 = fh_1 = 0\}$ is the annihilator module. An analogous statement holds for H_Z with its QC vector (g_0, g_1) .

D. Closed-form prediction of the k -collapse for $W = \text{NE}^2\text{NE}^2\text{N}$

We now apply the framework to the case-study word

$$W = \text{NE}^2\text{NE}^2\text{N}, \quad P(W) = \{(0, 1), (1, 2), (3, 2), (4, 3), (5, 4), (7, 4), (8, 5)\}$$

as drawn in Fig. 3. For row alternation, the QC check vector (h_0, h_1) can be computed explicitly.

Example 4 (QC check vector for $\text{NE}^2\text{NE}^2\text{N}$ under row alternation). Using the bases (a_X, q_0, q_1) from Sec. VII A, one finds

$$h_0(u, v) = uv + u^2v + u^3v^2 + u^4v^2, \quad h_1(u, v) = 1 + u^2v + u^4v^2,$$

in the ring $R = \mathbb{F}_2[u^{\pm 1}, v^{\pm 1}]/(u^{L_x/2} - 1, v^{L_y/2} - 1)$.

Proof. We list the offsets $Q \in P(W)$ and determine whether $a_X + Q$ lands in the q_0 or q_1 data coset. A direct parity check shows

$$a_X + (1, 2), a_X + (3, 2), a_X + (5, 4), a_X + (7, 4) \in q_0 + (2G_0),$$

$$a_X + (0, 1), a_X + (4, 3), a_X + (8, 5) \in q_1 + (2G_0).$$

Writing each target uniquely as $q_\sigma + (2\delta_x, 2\delta_y)$ produces the exponents

$$(1, 2) \mapsto u^1 v^1, (3, 2) \mapsto u^2 v^1, (5, 4) \mapsto u^3 v^2, (7, 4) \mapsto u^4 v^2$$

for h_0 , and

$$(0, 1) \mapsto 1, (4, 3) \mapsto u^2 v^1, (8, 5) \mapsto u^4 v^2$$

for h_1 , yielding the stated polynomials. \square

The key simplification is that h_0 has *paired* v -exponents, so it is annihilated by the “sum over all u ” idempotent.

Definition 6 (Horizontal sum idempotent). Let

$$S_u := 1 + u + u^2 + \dots + u^{L_x/2-1} \in R.$$

Then $u^t S_u = S_u$ for all t , so S_u is invariant under horizontal shifts.

Lemma 2 (A universal annihilation of h_0). *For the case-study word, $S_u h_0 = 0$ in R for every (L_x, L_y) . Moreover,*

$$S_u h_1 = S_u (1 + v + v^2).$$

Therefore, X -check dependencies are exactly controlled by the 1D cyclotomic factor $1 + v + v^2$ and its interaction with the vertical period $v^{L_y/2} - 1$.

Theorem 3 (Exact k -collapse criterion for row alternation). *Let $W = NE^2 NE^2 N$ and use the row-alternating layout on $G = \mathbb{Z}_{L_x} \times \mathbb{Z}_{L_y}$. Assume L_x, L_y are even so the checkerboard model is well-defined. Then*

$$\dim \ker(H_X^\top) = \deg \gcd(1 + v + v^2, v^{L_y/2} - 1), \quad \dim \ker(H_Z^\top) = \deg \gcd(1 + v + v^2, v^{L_y/2} - 1),$$

and hence

$$k = 2 \deg \gcd(1 + v + v^2, v^{L_y/2} - 1).$$

In particular, $k = 4$ if $3 \mid (L_y/2)$ (equivalently $6 \mid L_y$), and $k = 0$ otherwise.

Remark 5 (Interpretation of Table III). Theorem 3 explains the observed alternation of k in Table III without constructing H_X, H_Z explicitly. For thin rectangles $(L_x, L_y) = (2d, d)$ one has $L_y/2 = d/2$, so $k = 4$ exactly when $3 \mid (d/2)$, i.e. $6 \mid d$. This is precisely the commensurability mechanism that also stabilizes k on the $(12m, 6m)$ family.

VIII. ENUMERATION AND CANONICALIZATION OF COSET-CONSTANT LAYOUTS

Theorem 1 states that commutation-compatible layouts are constant on cosets of the odd-multiplicity lattice $L(W)$. This section makes that freedom explicit: it counts coset-constant layouts, describes natural equivalences (global $X \leftrightarrow Z$ and translations), and gives a canonical representative rule that supports reproducible layout scans.

A. Layouts as \mathbb{F}_2 -labelings of ancilla cosets

Fix a word W and assume (L_x, L_y) are such that the image of $L(W)$ in the torus is a subgroup that preserves the ancilla sublattice. Let $\mathcal{C}_A(W)$ denote the finite set of ancilla cosets:

$$\mathcal{C}_A(W) := \Lambda_A / L(W), \quad c := |\mathcal{C}_A(W)|.$$

A coset-constant layout is equivalently a function

$$\alpha : \mathcal{C}_A(W) \rightarrow \{X, Z\} \cong \mathbb{F}_2.$$

Proposition 6 (Raw layout count). *The number of commutation-compatible coset-constant layouts on Λ_A equals 2^c . Modulo the global swap $X \leftrightarrow Z$, the number of distinct layouts equals 2^{c-1} .*

Example 5 (Two- and four-coset words). If $L(W) = 2\mathbb{Z} \times 2\mathbb{Z}$, then $c = 2$ (Fig. 5, left), so there is only one nontrivial layout up to the global swap: one coset is X and the other is Z . If $L(W) = \text{span}\{(4, 0), (2, 2)\}$, then $c = 4$ (Fig. 5, right), giving $2^{4-1} = 8$ layouts up to global swap.

B. Translation equivalence and canonical representatives

Even when two layouts are different as functions on $\mathcal{C}_A(W)$, they can yield isomorphic codes if one is obtained from the other by a translation symmetry of the torus that preserves W (equivalently, preserves the pattern up to a translate). Such equivalences matter for searches: scanning all 2^{c-1} layouts may be redundant.

Let \mathcal{T} be the subgroup of even translations of G (those preserving Λ_A) that act on $\mathcal{C}_A(W)$ by permuting cosets. (Concretely, $\tau \in \mathcal{T}$ sends the coset of a to the coset of $a + \tau$.)

Proposition 7 (Translation-equivalent layouts yield isomorphic codes). *If two coset-constant layouts α, α' satisfy $\alpha' = \alpha \circ \pi$ for some coset permutation π induced by a translation of the torus, then the resulting CSS codes are isomorphic by a qubit relabeling (translation of coordinates).*

Definition 7 (Canonical layout representative). Fix an ordering of the cosets in $\mathcal{C}_A(W)$ (e.g. lexicographic by a chosen coset representative). Given a layout α , define $\text{can}(\alpha)$ as follows: apply every translation-induced coset permutation in \mathcal{T} to α , then (if desired) apply the global flip so that the first coset is labeled X , and finally choose the lexicographically smallest bitstring among the resulting layouts.

Remark 6 (Practical use in searches). Definition 7 is a concrete, implementation-friendly way to avoid redundant layout scans. In a script, one simply generates all 2^{c-1} labelings, canonicalizes each, and keeps one representative per canonical string.

IX. ROW-PERIODIC QUASI-CYCLIC REDUCTION VIA ANNIHILATORS

We now add a refinement of the quasi-cyclic viewpoint tailored to common layouts (especially row alternation): for a 2×2 unit cell, rank deficiency and stabilizer dependencies reduce to annihilators in a small polynomial ring.

A. The 2×2 unit cell and group algebra

Assume L_x, L_y even and define the reduced torus

$$G_0 := \mathbb{Z}_{L_x/2} \times \mathbb{Z}_{L_y/2}.$$

Let

$$R := \mathbb{F}_2[X^{\pm 1}, Y^{\pm 1}] / (X^{L_x/2} - 1, Y^{L_y/2} - 1)$$

be the group algebra of G_0 .

Row-periodic layouts (including row alternation) yield block-circulant check matrices generated by constant-size polynomial rows. For row alternation, there is one X -check type and one Z -check type per cell, represented by

$$\mathbf{h}_X = (h_{X,0}, h_{X,1}) \in R^{1 \times 2}, \quad \mathbf{h}_Z = (h_{Z,0}, h_{Z,1}) \in R^{1 \times 2},$$

where the two components correspond to the two data-qubit types per cell.

B. Annihilators and stabilizer dependencies

Definition 8 (Annihilator). For $\mathbf{h} = (h_0, h_1) \in R^{1 \times 2}$, define

$$\text{Ann}(\mathbf{h}) := \{f \in R : fh_0 = 0 \text{ and } fh_1 = 0\}.$$

D		C		D		C	
	A		B		A		B
C		D		C		D	
	B		A		B		A
D		C		D		C	
	A		B		A		B

FIG. 9. Ancilla cosets for $L(W) = \text{span}\{(4, 0), (2, 2)\}$ for the case-study word $W = \text{NE}^2\text{NE}^2\text{N}$. Two ancillas (x, y) and (x', y') lie in the same $L(W)$ -coset iff the pair of residues $(y \bmod 2, (x - y) \bmod 4)$ matches. Any commutation-compatible layout must be constant on each labeled class (Theorem 1), but the assignment of X versus Z across A–D is otherwise free up to global symmetries.

Proposition 8 (Rank deficiency from annihilators). *Let H be the block-circulant matrix over \mathbb{F}_2 generated by translating $\mathbf{h} \in R^{1 \times 2}$ over G_0 . Then $\dim_{\mathbb{F}_2} \ker(H^\top) = \dim_{\mathbb{F}_2} \text{Ann}(\mathbf{h})$ and*

$$\text{rank}(H) = |G_0| - \dim_{\mathbb{F}_2} \text{Ann}(\mathbf{h}).$$

Corollary 1 (A k -formula for row alternation). *In the row-alternating layout (one check type per cell for each Pauli type),*

$$k = \dim_{\mathbb{F}_2} \text{Ann}(\mathbf{h}_X) + \dim_{\mathbb{F}_2} \text{Ann}(\mathbf{h}_Z).$$

X. WORKED FAMILIES AND A DETAILED CASE STUDY

This section illustrates how the framework is used in practice:

$$W \longrightarrow P(W) \longrightarrow L(W) \longrightarrow \text{layout class} \longrightarrow \text{finite-torus behavior.}$$

A. Benchmark words through the invariant lens

The words NE^2N , NE^3N , $\text{N}^2\text{E}^2\text{N}^2$, and $\text{N}^2\text{E}^3\text{N}^2$ are central in [1]. Table I highlights a structural distinction: NE^2N and $\text{N}^2\text{E}^2\text{N}^2$ have $L(W) = 2\mathbb{Z} \times 2\mathbb{Z}$ (two ancilla cosets), while NE^3N and $\text{N}^2\text{E}^3\text{N}^2$ have $L(W) = \text{span}\{(4, 0), (2, 2)\}$ (four ancilla cosets). The latter class admits more layout freedom (Fig. 5), which is often useful when searching for good finite-size instances.

B. Case study: the word $W = \text{NE}^2\text{NE}^2\text{N}$ and its four cosets

We now focus on

$$W = \text{NE}^2\text{NE}^2\text{N} = \text{NEEENEEN},$$

with support pattern shown in Fig. 3. From Table I,

$$L(W) = \text{span}_{\mathbb{Z}}\{(4, 0), (2, 2)\}, \quad (20)$$

so layouts must be constant on four ancilla cosets.

A useful explicit coset invariant is the residue pair

$$(y \bmod 2, (x - y) \bmod 4), \quad (21)$$

which is constant on each $L(W)$ -coset. On ancilla sites $(x + y \text{ odd})$ this yields exactly four classes, labeled A–D in Fig. 9. Row alternation uses only $y \bmod 2$, while general coset-constant layouts may depend on both residues.

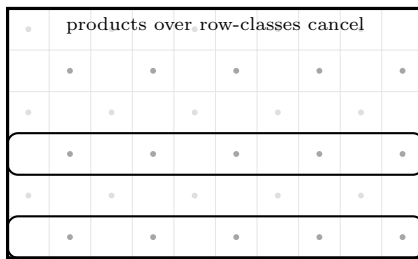


FIG. 10. Illustration of Proposition 9: on commensurate tori, products of checks over entire residue classes of anchor rows can cancel, producing stabilizer dependencies (formalized in Appendix O).

C. A structured torus family and certified nonzero k

We study the family $G_m = \mathbb{Z}_{12m} \times \mathbb{Z}_{6m}$ with the row-alternating layout (Fig. 1). Then $n = \frac{1}{2}(12m)(6m) = 36m^2$. In this family we can certify nonzero k by explicit stabilizer dependencies and exhibit explicit commuting operators that upper-bound distance.

Proposition 9 (Two stabilizer dependencies per type on $12m \times 6m$). *On G_m with the row-alternating layout, there exist two independent \mathbb{F}_2 relations among the X -checks and two among the Z -checks. Consequently,*

$$\text{rank}(H_X) \leq \#\Lambda_X - 2, \quad \text{rank}(H_Z) \leq \#\Lambda_Z - 2,$$

and therefore $k \geq 4$ for all m .

The dependencies are not mysterious algebraic accidents: they come from parity cancellations that are visible at the level of the word. Very roughly, when one multiplies (adds over \mathbb{F}_2) all X -checks whose anchors lie in certain y -residue classes modulo 6, each data qubit is hit an even number of times because the y -coordinates in $P(W)$ come in repeated pairs mod 6. This is why the same word on an incommensurate height can lose those dependencies and collapse to $k = 0$ under the same row-alternating layout (as seen in the thin-rectangle examples of Sec. XI): the torus no longer supports the residue-class partition underlying the cancellation. Fig. 10 shows this case.

D. An explicit commuting-operator motif

Let $t = (12, 6)$ and $r = (4, 2)$ modulo $(12m, 6m)$. For a data site $p \in \Lambda_Q$, define

$$S(p) = \{p + jt, p + r + jt : j = 0, 1, \dots, m-1\}. \quad (22)$$

Geometrically, $S(p)$ consists of two interleaved length- m orbits under translation by t , separated by the fixed displacement r (Fig. 11). The usefulness of this construction is that checking commutation reduces to an overlap-parity count between $S(p)$ and translated copies of $P(W)$; for suitable p , each check intersects $S(p)$ in an even number of sites.

Proposition 10 (Weight- $2m$ commuting operators). *For suitable choices of p , the Pauli operators X supported on $S(p)$ and Z supported on $S(p)$ commute with all opposite-type checks. In particular, for this family $d \leq 2m$.*

E. Exact criterion for dimension collapse on thin rectangles

A central practical phenomenon is boundary-condition sensitivity of k under a fixed word and layout. For the case-study word and row alternation on thin rectangles $(L_x, L_y) = (2d, d)$, the observed behavior admits an exact divisibility criterion.

Theorem 4 (Exact k -collapse criterion for $W = \text{NE}^2\text{NE}^2\text{N}$). *Let $W = \text{NE}^2\text{NE}^2\text{N}$ and consider the directional CSS instance on $(L_x, L_y) = (2d, d)$ with d even and the row-alternating layout. Then*

$$k = \begin{cases} 4, & 6 \mid d, \\ 0, & 6 \nmid d. \end{cases}$$

The proof uses the annihilator reduction from Section IX and is given in compressed form in Appendix Q.

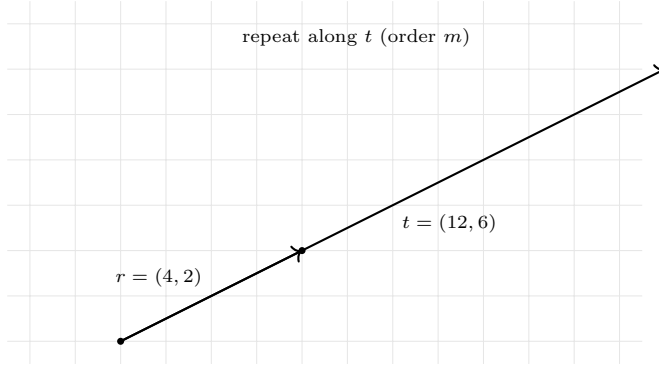


FIG. 11. The (r, t) motif in Proposition 10: two sites per step along a length- m orbit, giving weight $2m$ and hence a linear-in- m distance upper bound.

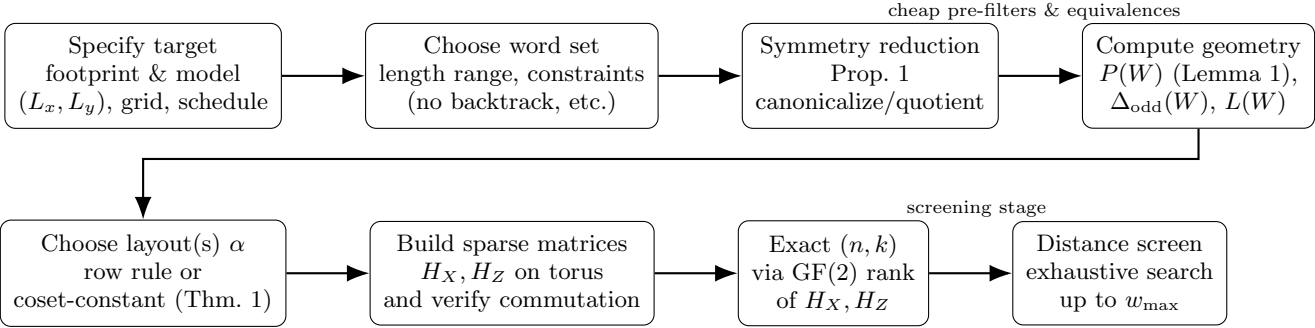


FIG. 12. Reproducible pipeline used in Sec. XI. The workflow is identical for validating a fixed (W, L_x, L_y, α) instance or for searching over many words. A practical search runs cheap filters and symmetry quotienting early, computes (n, k) exactly, and uses a small-weight distance screen to build a shortlist before investing in deeper distance calculations or broader layout/boundary scans.

XI. NUMERICAL EXPERIMENTS AND WORD SEARCH

This section explains numerical-results obtained in a reproducible way and how to interpret the kinds of finite-size effects that arise for route-generated, translation-invariant codes. The aim is not to claim best-in-class performance for the illustrative examples, but to provide a repeatable baseline for (i) validating a proposed word/layout instance and (ii) searching for promising new words under a fixed footprint and connectivity model. Throughout we emphasize that the quantities reported here are *static* code parameters of the CSS check matrices; circuit-level performance and thresholds require an explicit extraction circuit and a decoder model, which are outside our present scope.

A. Reproducible workflow for validation and word search.

For a fixed (W, L_x, L_y, α) , we build sparse H_X, H_Z , verify commutation ($H_X H_Z^\top = 0$), compute (n, k) exactly by rank over \mathbb{F}_2 , and estimate d_X, d_Z by exhaustive search up to a cutoff weight w_{\max} . If no nontrivial logical is found up to w_{\max} , we report $d > w_{\max}$. In practice, the exhaustive search cost grows quickly with n and w_{\max} , so entries of the form $d > w_{\max}$ should be read as *screening lower bounds* rather than definitive distances. A typical workflow is to use a small cutoff to shortlist candidates and then rerun only the shortlist with higher cutoffs or specialized distance routines. The end-to-end workflow used to generate the tables in this section is summarized in Fig. 12.

All tables were generated using a companion script [30]. The script parses compressed words (e.g. $\mathbf{NE}^2\mathbf{N}^2\mathbf{E}^2\mathbf{N}$), constructs $P(W)$ from Lemma 1, builds H_X, H_Z on the checkerboard torus, and runs small-weight searches. The same script can enumerate words up to symmetry using Proposition 1 and can filter by simple route constraints (no immediate backtracking, distinct offsets, and/or “full support” without cancellations). We stress that the tables below use the *row-alternating* layout for concreteness; for words whose odd-difference lattice has more than two ancilla cosets (e.g. $L(W) = \text{span}\{(4, 0), (2, 2)\}$ in Table I), it is often beneficial to also enumerate all coset-constant layouts allowed

TABLE II. Case-study family $W = \text{NE}^2\text{NE}^2\text{N}$ on $12m \times 6m$ tori (row-alternating layout). Entries $d > 3$ mean no nontrivial logical of weight ≤ 3 was found, so $d \geq 4$.

m	$L_x \times L_y$	n	k	d_X	d_Z
1	12×6	36	4	2	2
2	24×12	144	4	4	4
3	36×18	324	4	> 3	> 3

TABLE III. Dimension collapse for $W = \text{NE}^2\text{NE}^2\text{N}$ on thin rectangles $(L_x, L_y) = (2d, d)$ (row-alternating layout).

d	$L_x \times L_y$	n	k
6	12×6	36	4
8	16×8	64	0
10	20×10	100	0
12	24×12	144	4
14	28×14	196	0
18	36×18	324	4

by Theorem 1 and repeat the same screening procedure.

B. Case study family and its scaling signals.

For $W = \text{NE}^2\text{NE}^2\text{N}$ on $12m \times 6m$ tori with row alternation, Table II summarizes (n, k) and distance searches. Two trends are worth highlighting. First, the observed constant $k = 4$ across $m = 1, 2, 3$ is consistent with the analytical stabilizer-dependency mechanism established earlier: Proposition 9 guarantees two independent dependencies among the X -checks and two among the Z -checks on this commensurate torus family, yielding $k \geq 4$ for all m . In other words, the *dimension is protected* by a structural dependency that is robust under scaling along $(12m, 6m)$, not a coincidence of small size. Second, the distances for $m = 1, 2$ saturate the explicit commuting-operator construction: Proposition 10 gives a family of weight- $2m$ commuting operators, hence $d \leq 2m$, while Table II shows $d_X = d_Z = 2m$ for $m = 1, 2$. For $m = 3$ the table only reports $d_X, d_Z > 3$ because the search cutoff was $w_{\max} = 3$; combining this with Proposition 10 yields the informative bracket $4 \leq d \leq 6$ for $m = 3$. A natural next numerical step (and one we recommend when reporting this family on larger footprints) is to increase w_{\max} for this single word on the structured tori to test the working hypothesis suggested by the first two points, namely that $d = 2m$ may hold along $(12m, 6m)$ for this layout.

C. Boundary-condition sensitivity as a design constraint.

Keeping the same word and layout but changing boundary conditions can collapse k . Table III illustrates this for thin rectangles $(L_x, L_y) = (2d, d)$, where $n = d^2$ makes the footprint attractive. The striking feature is that k alternates between 4 and 0 as d changes: $k = 4$ for $d = 6, 12, 18$ but $k = 0$ for $d = 8, 10, 14$ under the same row-alternating layout. This is a concrete instance of a familiar quasi-cyclic phenomenon: for translation-invariant codes, the ranks of H_X and H_Z (hence k) can depend strongly on the torus periods. Here the effect has a particularly simple interpretation. The stabilizer dependencies that certify $k \geq 4$ on $(12m, 6m)$ are built from cancellations over residue classes modulo 6 in the vertical coordinate (Appendix O); these cancellations close consistently only when L_y is a multiple of 6. When L_y is not divisible by 6, those specific global dependencies disappear, the check matrices become full-rank in the relevant sense, and the resulting code encodes no logical qubits ($k = 0$). Rather than viewing such instances as failures, Table III should be read as a practical message for hardware-driven design: *boundary conditions are part of the code specification* for route-generated quasi-cyclic constructions, and one should scan over (L_x, L_y) (or over allowed shear/quotient choices) rather than fixing a single aspect ratio and assuming the dimension will be stable. It also motivates exploring alternative allowed layouts beyond row alternation: because $W = \text{NE}^2\text{NE}^2\text{N}$ has $L(W) = \text{span}\{(4, 0), (2, 2)\}$, Theorem 1 permits a four-coset family of layouts, some of which can restore $k > 0$ on sizes where the row-alternating layout collapses.

TABLE IV. Top candidates from a scan on the 16×8 torus (row-alternating layout). Entries $d > 4$ mean no nontrivial logical of weight ≤ 4 was found, so $d \geq 5$.

word W	w	n	k	d_X	d_Z
NES ² EN	6	64	6	> 4	> 4
NE ² N ² E ² N	8	64	18	4	4
N ² ENW ² NE	8	64	10	4	4
N ² ESW ² SE	8	64	10	4	4
N ³ E ² NW ²	8	64	10	4	4
NENE ² NEN	8	64	10	4	4
NENENWNW	8	64	10	4	4
NENESWSW	8	64	10	4	4
N ² E ² N ²	6	64	6	4	4
NENW ² NES	8	64	6	4	4

D. Understanding the Search Table: Insights and Limitations.

To show how a “new code search” can be documented, we scanned words of length $4 \leq w \leq 8$ on the 16×8 torus, quotiented by symmetry (fixing the first letter N), disallowing immediate backtracking, and keeping only commuting CSS instances under row alternation. Table IV lists the top candidates found under this setting. The goal here is not to optimize a single metric, but to illustrate what a transparent reporting pipeline looks like and what kinds of tradeoffs appear even at modest sizes.

A first observation is that a fixed footprint can admit many distinct commuting words with markedly different *dimension* k at the same n . For example, NE²N²E²N attains $k = 18$ at $n = 64$, while several other length-8 words yield $k = 10$ or $k = 6$. High k at fixed n typically reflects additional stabilizer dependencies (fewer independent checks), and in quasi-cyclic settings such dependencies are often tied to symmetry and commensurability effects similar to those seen in Table III. A second observation is that the reported distances for most candidates are modest ($d_X = d_Z = 4$ under the cutoff), while NES²EN stands out with $d_X, d_Z > 4$ at the chosen cutoff, making it a natural candidate for deeper distance tests. At the same time, one should be cautious in over-interpreting the distance column at this stage: for entries with $d > 4$ the true distance could be 5 or substantially larger, and conversely distance can change under different layouts or boundary choices. This is why we recommend a two-stage procedure: use tables like Table IV to shortlist, then rerun the shortlist with larger w_{\max} and with additional allowed layouts (coset-constant layouts from Theorem 1) to check robustness.

Finally, the support-pattern sketches in Fig. 13 provide geometric intuition about why very different words can survive the same footprint and layout filter. The examples include both “snake-like” patterns and patterns with pronounced turns or near-loops; empirically, these geometric features correlate with how often translated checks overlap and therefore with the likelihood of additional dependencies and/or short logical operators. From an implementation perspective, there is also a direct engineering tradeoff hidden behind the word length w : longer words correspond to deeper per-check measurement schedules (more two-qubit interactions), which may hurt circuit-level performance even if the static parameters look attractive. For this reason, when using Table IV as a discovery tool, we recommend reporting w together with the effective support size $|P(W)|$ (which may be smaller than w if offsets cancel modulo 2), and treating short, robust-to-boundaries candidates as especially valuable starting points for circuit-level studies.

XII. SUMMARY AND OUTLOOK

Directional codes provide a concrete route to low-connectivity qLDPC instances by enforcing that each stabilizer is generated by a short, hardware-compatible route [1]. A central takeaway of this paper is that many structural features are visible directly at the level of the word: Lemma 1 makes the route-to-support map explicit, and Theorem 1 organizes admissible layouts through a computable lattice $L(W)$. Beyond repackaging these foundations, we added three analysis tools aimed at practical design: (i) a formal equivalence/canonicalization theory for removing redundancy in word scans (Sec. IV); (ii) an inverse-problem criterion separating route-realizable patterns from generic translation-invariant ones (Sec. V); and (iii) a quasi-cyclic annihilator reduction explaining boundary-condition sensitivity of k under row-periodic layouts (Sec. IX), culminating in an exact k -collapse theorem for the case-study word (Theorem 4). These tools complement numerical exploration and can guide footprint/layout choices before expensive circuit-level simulations.

Natural next steps include systematic enumeration of coset-constant layouts (not only row alternation), sharper

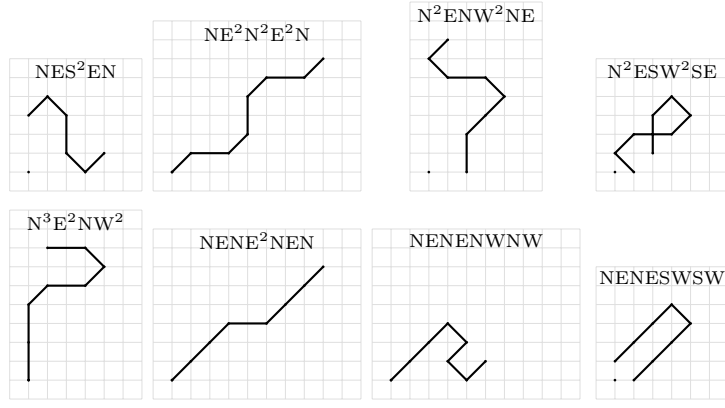


FIG. 13. Support patterns $P(W)$ for a subset of the top candidates in Table IV.

admissibility tests tailored to specific extraction schedules, and circuit-level evaluation using hardware-aware tools [28, 31] and fast stabilizer simulation [32] with modern qLDPC decoders [33–36].

Appendix A: Proof of Lemma 1

Proof. Let the route positions be S_0, S_1, \dots, S_w with $S_j = \sum_{t=1}^j d_t$ and $S_0 = 0$. In the doubled-integer convention of [1], the j th interaction point is represented by the midpoint sum $Q_j = S_{j-1} + S_j$. Substituting $S_j = S_{j-1} + d_j$ yields $Q_j = 2S_{j-1} + d_j = 2\sum_{t=1}^{j-1} d_t + d_j$. \square

Appendix B: Proof of Theorem 1

Proof. Let $S_a = a + P(W)$ denote the support of the check anchored at a . For anchors a, b with $\delta = b - a$, we have $q \in S_a \cap S_b$ iff $q = a + Q_i = b + Q_j$ for some $Q_i, Q_j \in P(W)$, equivalently $\delta = Q_j - Q_i$. Thus $|S_a \cap S_b| \bmod 2$ equals $\mu(\delta) \bmod 2$ from the multiset $\Delta(W)$. If $\delta \in \Delta_{\text{odd}}(W)$, then the overlap is odd; hence a and b cannot be opposite types in a commuting CSS layout, so $\alpha(a) = \alpha(b)$ for all such δ . Closure under integer combinations implies α is constant on cosets of $L(W) = \text{span}_{\mathbb{Z}}(\Delta_{\text{odd}}(W))$.

Conversely, if α is constant on cosets of $L(W)$, then any odd-overlap displacement connects same-type anchors, so all opposite-type overlaps have even parity and the CSS commutation condition holds. \square

Appendix C: Proof of Proposition 1

Proof. A dihedral symmetry is a \mathbb{Z}^2 automorphism acting on the step vectors and thus on partial sums S_j and offsets $Q_j = S_{j-1} + S_j$, mapping $P(W)$ to an affine image. Reversal with inversion traverses the same geometric route in reverse time; it produces the same interaction set up to an overall translation. Cyclic shifts correspond to changing the start point along the same cycle, again translating $P(W)$. Thus $P(W')$ is an affine image of $P(W)$ under an automorphism and translation, which induces a qubit permutation and stabilizer relabeling on any compatible torus embedding. \square

Appendix D: Canonicalization under word equivalence

Let \mathcal{G} be the finite group generated by: the eight dihedral symmetries of the square acting on letters; reversal with inversion; and cyclic shifts. Given W , enumerate its orbit $\{g(W) : g \in \mathcal{G}\}$ (size at most $16w$). Define $\text{can}(W)$ to be the lexicographically smallest expanded-letter string in the orbit (ties broken deterministically). Then $W \sim W'$ iff $\text{can}(W) = \text{can}(W')$.

Appendix E: Proof of Proposition 2

Proof. If $W = d_1 \cdots d_w$ generates offsets $Q_j = S_{j-1} + S_j$, then $Q_1 = S_0 + S_1 = d_1 \in \mathcal{D}$. Moreover $Q_{j+1} - Q_j = d_j + d_{j+1} \in \Sigma$ (Eq. (14)), hence $d_{j+1} = (Q_{j+1} - Q_j) - d_j$, giving the recursion.

Conversely, assume $Q_1 \in \mathcal{D}$ and the recursion produces $d_j \in \mathcal{D}$. Define $S_0 = 0$ and $S_j = \sum_{t=1}^j d_t$. Inductively, $S_{j-1} + S_j = Q_j$ holds for $j = 1$. If $S_{j-1} + S_j = Q_j$, then using $S_{j+1} = S_j + d_{j+1}$ and $d_j + d_{j+1} = Q_{j+1} - Q_j$,

$$\begin{aligned} S_j + S_{j+1} &= S_j + (S_j + d_{j+1}) = (S_{j-1} + S_j) + (d_j + d_{j+1}) \\ &= Q_j + (Q_{j+1} - Q_j) = Q_{j+1}. \end{aligned}$$

Thus $Q_j = S_{j-1} + S_j$ for all j , so $P(W) = \{Q_j\}$ with the given order. Uniqueness follows from the recursion. \square

Appendix F: Proof of Proposition 3

Proof. A nonzero vector $v = (v_x, v_y)$ becomes 0 modulo (L_x, L_y) iff $L_x \mid v_x$ and $L_y \mid v_y$. If $|v_x| < L_x$ and $|v_y| < L_y$, this is impossible unless $v = 0$. Apply this to all vectors in $D(W) \cup (D(W) \pm D(W))$. \square

Appendix G: Proof of Proposition 4

Proof. A row of H_X anchored at $a_X + (2i, 2j)$ is a translate of the row anchored at a_X by the even vector $(2i, 2j)$. On the coarse group G_0 , this translation is exactly multiplication by $u^i v^j$. Each offset $Q \in P(W)$ contributes a 1 in the data coset $q_{\sigma(Q)}$ at displacement $\delta(Q)$, so the anchored row is encoded by $u^i v^j \cdot u^{\delta_x(Q)} v^{\delta_y(Q)}$ in that coset. Summing over Q and grouping by $\sigma(Q) \in \{0, 1\}$ yields the claim. \square

Appendix H: Proof of Proposition 5

Proof. Let $m_X = |\Lambda_X|$ and $m_Z = |\Lambda_Z|$ so $m_X + m_Z = n$. Then

$$\dim \ker(H_X^\top) = m_X - \text{rank}(H_X), \quad \dim \ker(H_Z^\top) = m_Z - \text{rank}(H_Z).$$

Substitute into $k = n - \text{rank}(H_X) - \text{rank}(H_Z)$ to obtain

$$k = n - (m_X - \dim \ker(H_X^\top)) - (m_Z - \dim \ker(H_Z^\top)) = \dim \ker(H_X^\top) + \dim \ker(H_Z^\top).$$

\square

Appendix I: Proof of Theorem 2

Proof. By Proposition 4, any GF(2) linear combination of X -checks with coefficient pattern $f \in R$ produces the data-vector $(fh_0, fh_1) \in R \oplus R$. Such a combination is a stabilizer dependency if and only if the resulting data-vector is the zero vector, i.e. $fh_0 = fh_1 = 0$ in R . The identification with $\ker(H_X^\top)$ follows from the standard correspondence between left-kernel vectors and GF(2) relations among rows. \square

Appendix J: Proof of Lemma 2

Proof. Using Example 4,

$$S_u h_0 = S_u(uv + u^2v + u^3v^2 + u^4v^2).$$

Since $u^t S_u = S_u$, each term satisfies $S_u u^t = S_u$, hence

$$S_u h_0 = S_u(v + v + v^2 + v^2) = S_u \cdot 0 = 0.$$

Similarly,

$$S_u h_1 = S_u(1 + u^2v + u^4v^2) = S_u(1 + v + v^2).$$

\square

Appendix K: Proof of Theorem 3

Proof. By Theorem 2, $\ker(H_X^\top)$ corresponds to the annihilator $\text{Ann}_R(h_0, h_1)$. Lemma 2 shows that any element of the form $S_u \cdot f(v)$ annihilates h_0 , and annihilates h_1 if and only if

$$(S_u f(v)) h_1 = S_u f(v) (1 + v + v^2) = 0.$$

Because $S_u \neq 0$ and generates a 1-dimensional ideal in the u -direction, the dimension of such annihilators is exactly the dimension of

$$\ker(\cdot (1 + v + v^2) : \mathbb{F}_2[v^{\pm 1}]/(v^{L_y/2} - 1) \rightarrow \mathbb{F}_2[v^{\pm 1}]/(v^{L_y/2} - 1)).$$

For a circulant multiplication operator, this kernel dimension equals $\deg \gcd(1 + v + v^2, v^{L_y/2} - 1)$. Thus $\dim \ker(H_X^\top)$ equals this degree. The Z -type statement follows by symmetry (the same word and the complementary ancilla coset yield the same vertical factor). Finally, Proposition 5 gives $k = \dim \ker(H_X^\top) + \dim \ker(H_Z^\top)$.

The final criterion uses the classical fact that $1 + v + v^2$ divides $v^M - 1$ over \mathbb{F}_2 if and only if $3 \mid M$. Hence $k = 2 \cdot 2 = 4$ when $3 \mid (L_y/2)$ and $k = 0$ otherwise. \square

Appendix L: Proof of Proposition 6

Proof. Each of the c cosets may be labeled independently by X or Z , giving 2^c layouts. The global swap identifies each labeling with its bitwise complement, so the quotient count is $2^c/2 = 2^{c-1}$. \square

Appendix M: Proof of Proposition 7

Proof. A translation of the lattice relabels both ancilla anchors and data qubits. Because each check support is a translate of $P(W)$, translating the entire construction preserves the check pattern and sends the layout α to the permuted layout α' . This induces an isomorphism of the resulting stabilizer groups and hence of the CSS code. \square

Appendix N: Proof of Proposition 8

Proof. Identify $\mathbb{F}_2^{2|G_0|}$ with R^2 by mapping each data-type configuration to its group-algebra element, and identify the set of translated check rows with R . Translation corresponds to multiplying \mathbf{h} by a monomial, so the row span is the R -submodule $R\mathbf{h} \subset R^2$. A dependency among translated rows is exactly an $f \in R$ with $f\mathbf{h} = 0$, i.e. $f \in \text{Ann}(\mathbf{h})$. Thus $\ker(H^\top) \cong \text{Ann}(\mathbf{h})$ and $\text{rank}(H) = |G_0| - \dim \text{Ann}(\mathbf{h})$. \square

Appendix O: Proof of Proposition 9

Proof. We prove the X -check statement; the Z -check statement is identical by symmetry. In the row-alternating layout on $G_m = \mathbb{Z}_{12m} \times \mathbb{Z}_{6m}$, X -ancillas occupy even- y ancilla rows. Consider the $\text{GF}(2)$ sum of all X -checks anchored at ancillas with $y \equiv 0$ or $2 \pmod{6}$. A data qubit $q = (x, y) \in \Lambda_Q$ appears in an X -check anchored at a iff $a = q - Q_j$ for some $Q_j \in P(W)$. Hence q appears in the chosen sum exactly

$$\#\{j : y - (Q_j)_y \equiv 0 \text{ or } 2 \pmod{6}\}$$

times. For $W = \text{NE}^2\text{NE}^2\text{N}$, the multiset of $(Q_j)_y$ is $\{1, 2, 2, 3, 4, 4, 5\}$, and a direct residue check over \mathbb{Z}_6 shows the count is always even; thus the sum is the zero row, giving one dependency. Similarly, summing over anchors with $y \equiv 0$ or $4 \pmod{6}$ gives a second dependency. These are independent because their symmetric difference is nonempty. Thus $\text{rank}(H_X) \leq \#\Lambda_X - 2$. Repeating for Z yields $\text{rank}(H_Z) \leq \#\Lambda_Z - 2$, and since $\#\Lambda_X + \#\Lambda_Z = n$ we obtain $k \geq 4$. \square

Appendix P: Proof of Proposition 10

Proof. Let $S(p) = \{p + jt, p + r + jt\}_{j=0}^{m-1}$ with $t = (12, 6)$ and $r = (4, 2)$. Because t has order m on $\mathbb{Z}_{12m} \times \mathbb{Z}_{6m}$, $S(p)$ is the union of two length- m orbits. Fix an opposite-type check anchored at a with support $a + P(W)$. The overlap

parity $|(a + P(W)) \cap S(p)| \bmod 2$ depends only on residues along the t -orbits; using the same $\{1, 2, 2, 3, 4, 4, 5\}$ residue structure as in Appendix O, one checks that for suitable p every such overlap is even. Thus the corresponding Pauli commutes with all opposite-type checks. \square

Appendix Q: Proof of Theorem 4

Proof. Consider $(L_x, L_y) = (2d, d)$ with d even and row alternation. Then $G_0 = \mathbb{Z}_d \times \mathbb{Z}_{d/2}$ and

$$R = \mathbb{F}_2[X^{\pm 1}, Y^{\pm 1}]/(X^d - 1, Y^{d/2} - 1).$$

By Corollary 1, $k = \dim \text{Ann}(\mathbf{h}_X) + \dim \text{Ann}(\mathbf{h}_Z)$.

A direct cell-type computation for $W = \text{NE}^2\text{NE}^2\text{N}$ yields polynomial rows

$$\mathbf{h}_X = (h_{X,0}, h_{X,1}),$$

$$h_{X,1} = 1 + V + V^2, \quad h_{X,0} = (1 + X)XY(1 + V),$$

and

$$\mathbf{h}_Z = (h_{Z,0}, h_{Z,1}),$$

$$h_{Z,0} = Y(1 + V + V^2), \quad h_{Z,1} = Y(1 + X)(1 + V),$$

where $V := X^2Y$ and XY is a unit in R .

Let $f \in \text{Ann}(\mathbf{h}_X)$, so $fh_{X,0} = fh_{X,1} = 0$. Since XY is a unit and $\gcd(1 + V, 1 + V + V^2) = 1$ in $\mathbb{F}_2[V]$, these two equations imply $f(1 + X) = 0$. In $\mathbb{F}_2[X]/(X^d - 1)$, the annihilator of $(1 + X)$ is the ideal generated by

$$S_X := 1 + X + \cdots + X^{d-1},$$

because $(1 + X)S_X = 1 + X^d = 0$. Hence $f = S_X g$ for some $g \in R$; moreover $S_X X^t = S_X$ forces g to depend only on Y , i.e. $f = S_X g(Y)$. Then $fh_{X,1} = 0$ reduces to

$$g(Y)(1 + Y + Y^2) = 0 \quad \text{in} \quad \mathbb{F}_2[Y]/(Y^{d/2} - 1).$$

Thus $\text{Ann}(\mathbf{h}_X) \neq \{0\}$ iff $1 + Y + Y^2$ divides $Y^{d/2} - 1$, i.e. iff $3 \mid (d/2)$. In that case $\dim \text{Ann}(\mathbf{h}_X) = 2$ (a standard cyclic-code count for the $(1 + Y + Y^2)$ -annihilator in length- $d/2$).

The same argument applies to \mathbf{h}_Z (the roles of the components swap but the common factor $1 + V + V^2$ is unchanged), yielding $\dim \text{Ann}(\mathbf{h}_Z) = \dim \text{Ann}(\mathbf{h}_X)$. Therefore

$$k = \begin{cases} 4, & 3 \mid (d/2) \Leftrightarrow 6 \mid d, \\ 0, & \text{otherwise.} \end{cases}$$

\square

-
- [1] G. P. Gehér, D. Byfield, and A. Ruban, Directional codes: a new family of quantum LDPC codes on hexagonal- and square-grid connectivity hardware (2025), arXiv:2507.19430.
 - [2] P. W. Shor, Scheme for reducing decoherence in quantum computer memory, Phys. Rev. A **52**, R2493 (1995).
 - [3] A. R. Calderbank and P. W. Shor, Good quantum error-correcting codes exist, Phys. Rev. A **54**, 1098 (1996).
 - [4] A. M. Steane, Error correcting codes in quantum theory, Phys. Rev. Lett. **77**, 793 (1996).
 - [5] D. Gottesman, Stabilizer codes and quantum error correction (1997), arXiv:quant-ph/9705052.
 - [6] R. G. Gallager, *Low-Density Parity-Check Codes* (MIT Press, 1962).
 - [7] R. M. Tanner, A recursive approach to low complexity codes, IEEE Trans. Inf. Theory **27**, 533 (1981).
 - [8] D. J. C. MacKay, Good error-correcting codes based on very sparse matrices, IEEE Trans. Inf. Theory **45**, 399 (1999).

- [9] D. J. C. MacKay, G. Mitchison, and P. L. McFadden, Sparse graph codes for quantum error correction, *IEEE Trans. Inf. Theory* **50**, 2315 (2004).
- [10] B. M. Terhal, Quantum error correction for quantum memories, *Rev. Mod. Phys.* **87**, 307 (2015).
- [11] Error Correction Zoo, Quantum LDPC codes (online resource), <https://errorcorrectionzoo.org/list/qldpc> (2025), accessed 2026-02-06.
- [12] A. Y. Kitaev, Fault-tolerant quantum computation by anyons, *Annals of Physics* **303**, 2 (2003).
- [13] E. Dennis, A. Kitaev, A. Landahl, and J. Preskill, Topological quantum memory, *J. Math. Phys.* **43**, 4452 (2002).
- [14] A. G. Fowler, M. Mariantoni, J. M. Martinis, and A. N. Cleland, Surface codes: Towards practical large-scale quantum computation, *Phys. Rev. A* **86**, 032324 (2012).
- [15] S. Bravyi, D. Poulin, and B. M. Terhal, Tradeoffs for reliable quantum information storage in 2d systems, *Phys. Rev. Lett.* **104**, 050503 (2010).
- [16] S. Bravyi and B. M. Terhal, A no-go theorem for a two-dimensional self-correcting quantum memory based on stabilizer codes, *New J. Phys.* **11**, 043029 (2009).
- [17] J.-P. Tillich and G. Zémor, Quantum LDPC codes with positive rate and minimum distance proportional to the square root of the blocklength, *IEEE Trans. Inf. Theory* **60**, 1193 (2014).
- [18] A. Couvreur, N. Delfosse, and G. Zémor, Construction of quantum LDPC codes from cayley graphs, *IEEE Trans. Inf. Theory* **59**, 6087 (2013).
- [19] S. Bravyi and M. B. Hastings, Homological product codes, *Proceedings of STOC* (2014), arXiv:1311.0885.
- [20] A. Leverrier, J.-P. Tillich, and G. Zémor, Quantum expander codes, *FOCS* (2015), arXiv:1504.02882.
- [21] P. Panteleev and G. Kalachev, Asymptotically good quantum and locally testable classical LDPC codes (2021), arXiv:2111.03654.
- [22] P. Panteleev and G. Kalachev, Quantum LDPC codes with almost linear minimum distance, *IEEE Trans. Inf. Theory* (2022), arXiv:2012.04068.
- [23] M. B. Hastings, J. Haah, and R. O'Donnell, Fiber bundle codes: breaking the $n^{1/2}$ polylog(n) barrier for quantum LDPC codes (2021), arXiv:2009.03921.
- [24] N. P. Breuckmann and J. N. Eberhardt, Balanced product quantum codes, *PRX Quantum* **2**, 040101 (2021).
- [25] S. Bravyi, A. W. Cross, J. M. Gambetta, D. Maslov, P. Rall, and T. J. Yoder, High-threshold and low-overhead fault-tolerant quantum memory, *Nature* **627**, 778 (2024).
- [26] T. J. Yoder, E. Schoute, P. Rall, E. Pritchett, J. M. Gambetta, A. W. Cross, M. Carroll, and M. E. Beverland, Tour de gross: A modular quantum computer based on bivariate bicycle codes (2025), arXiv:2506.03094.
- [27] A. Shaw and B. M. Terhal, Lowering connectivity requirements for bivariate bicycle codes using morphing circuits, *Phys. Rev. Lett.* **134**, 090602 (2025), arXiv:2407.16336.
- [28] M. Mathews, L. Pahl, D. Pahl, V. L. Addala, C. Tang, W. D. Oliver, and J. A. Grover, Placing and routing quantum LDPC codes in multilayer superconducting hardware (2025), arXiv:2507.23011.
- [29] N. Berthussen, N. Delfosse, and M. E. Beverland, Toward a 2d local implementation of quantum LDPC codes, *PRX Quantum* **6**, 010306 (2025).
- [30] M. Rowshan, Directional qLDPC codes: Numerics, https://github.com/mohammad-rowshan/directional_qLDPC_codes (2026), gitHub repository.
- [31] Engineering Quantum Systems (EQuS), HAL: Hardware-aware layout (software), <https://github.com/EQuS/HAL> (2025), accessed 2026-02-06.
- [32] C. Gidney, Stim: a fast stabilizer circuit simulator (software), <https://github.com/quantumlib/Stim> (2021), accessed 2026-02-06.
- [33] D. Poulin and Y. R. Chung, On the iterative decoding of sparse quantum codes, *Quantum Inf. Comput.* **8**, 987 (2008), arXiv:0801.1241.
- [34] N. Delfosse and N. H. Nickerson, Almost-linear time decoding algorithm for topological codes (2017), arXiv:1709.06218.
- [35] J. Roffe, Decoding across the quantum LDPC code landscape (2020), arXiv:2005.07016.
- [36] S. Wolański and K. B. Barber, Ambiguity clustering: an accurate and efficient decoder for qLDPC codes (2024), arXiv:2406.14527.